

Sources of HO_x and production of ozone in the upper troposphere over the United States

L. Jaeglé,¹ D. J. Jacob,¹ W. H. Brune,² D. Tan,² I. C. Faloona,² A. J. Weinheimer,³
B. A. Ridley,³ T. L. Campos,³ G. W. Sachse⁴

Abstract. The sources of HO_x (OH+peroxy radicals) and the associated production of ozone at 8-12 km over the United States are examined by modeling observations of OH, HO₂, NO, and other species during the SUCCESS aircraft campaign in April-May 1996. The HO_x concentrations measured in SUCCESS are up to a factor of 3 higher than can be calculated from oxidation of water vapor and photolysis of acetone. The highest discrepancy was seen in the outflow of a convective storm. We show that convective injection of peroxides (CH₃OOH and H₂O₂) and formaldehyde (CH₂O) from the boundary layer to the upper troposphere could resolve this discrepancy. More generally, the data collected over the central United States during SUCCESS suggests that local convection was a major source of HO_x and NO_x to the upper troposphere. The OH and HO₂ observations together with the observations of NO allow us to directly calculate the ozone production in the upper troposphere and its dependence on NO_x. We find an average net ozone production of 2 ppbv day⁻¹ between 8 and 12 km over the continental United States in the spring. Ozone production was NO_x-limited under essentially all the conditions encountered in SUCCESS. The high levels of HO_x present in the upper troposphere stimulate ozone production and increase the sensitivity of ozone to NO_x emissions from aircraft and other sources.

Introduction

In the troposphere, ozone is produced by oxidation of CO and hydrocarbons in the presence of nitrogen oxide radicals (NO_x=NO+NO₂) and hydrogen oxide radicals (HO_x=OH+peroxy radicals). There is at present considerable interest in understanding the effects of increasing aircraft NO_x emissions on ozone in the upper troposphere [Schumann, 1995; NASA, 1997]. Depending on the relative supply of NO_x and HO_x in the upper troposphere, an increase in NO_x may cause either an increase or a decrease in ozone [Brasseur *et al.*, 1996].

In this paper we analyze the first concurrent measurements of HO_x [Brune *et al.*, this issue] and NO_x [Campos *et al.*, this issue] made in the aircraft flight corridor over the central United States. The measurements were made during the SUCCESS (SUBsonic aircraft: Cloud and Contrail Effects Special Study) DC-8 mission [Toon *et al.*, this issue]. We examine the factors controlling HO_x concentrations in the upper troposphere by comparing a photochemical model to the SUCCESS data. We use the combination of HO_x and NO_x measurements to quantify ozone production in the upper troposphere and assess its sensitivity to anthropogenic NO_x. A companion paper [Jaeglé *et al.*, this issue] focuses on the origin and chemical cycling of NO_x.

Model description

We use the Harvard 0-D photochemical model to calculate the concentrations of radicals and other photochemical intermediates along the aircraft flight tracks [Jacob *et al.*, 1996]. The model calculations are constrained with local 1-minute averaged observations of O₃, CO, NO, H₂O, CH₄, pressure, temperature, UV ra-

diation, and aerosol surface area. Acetone was not measured in SUCCESS but is included in our calculations as a linear function of CO concentrations based on the acetone-CO correlation observed in the PEM-West B aircraft campaign over the western Pacific [McKeen *et al.*, 1997]. The resulting acetone concentrations in the upper troposphere range from 200 to 900 pptv (average of 550 pptv). The values may be too low for a continental atmosphere, as sampled in SUCCESS, considering that acetone has a shorter lifetime than CO and that the acetone-CO correlation is based on relatively old marine air. The sensitivity of model results to the assumed concentration of acetone will be discussed below.

All input quantities except NO concentrations are assumed constant over the diel cycle. Total NO_x (= NO+NO₂+NO₃+2N₂O₅+HNO₂+HNO₄) is also assumed constant and is calculated iteratively in the model to match the observed NO at the time of day of observations. The model calculates the diel steady state concentrations of 30 species including HO₂, OH, O(¹D), CH₃O, CH₃O₂, NO_y species (NO₂, NO₃, N₂O₅, HNO₂, HNO₄, HNO₃, PAN), and other photochemical intermediates (H₂O₂, CH₃OOH, and CH₂O) along the flight track of the aircraft. "Diel steady state" is defined by the reproducibility of concentrations in the model over a 24-hour solar cycle. The corresponding 24-hour average reaction rates are also retrieved from the model output. Model calculations for a total of 2770 individual points were performed. The photochemical mechanism used in this model is the same as in Jacob *et al.* [1996], with updated rates [DeMore *et al.*, 1997]. For acetone photolysis we use recent measurements of the temperature-dependent cross-sections and pressure-dependent quantum yield [McKeen *et al.*, 1997].

The ozone column was specified from daily SBUV/2 satellite observations (A. J. Miller and C. Long, personal communication, 1996). Cloud and albedo effects are taken into account by using the NO₂ photolysis rate (JNO₂(Eppley)) derived from the Eppley UV radiometer instrument on-board the DC-8 [Madronich, 1987]. All the clear sky photolysis rates are scaled by JNO₂(Eppley)/JNO₂(clear), where JNO₂(clear) is the clear sky NO₂ photolysis rate computed by the radiation model at the local time of day of the observations (assuming a surface albedo of 0.1). For clear sky periods, JNO₂(Eppley) and JNO₂(clear) are within 10% of each other. Because the DC-8 often flew in the vicinity of clouds, the ratio of JNO₂(Eppley)/JNO₂(clear) ranged between 0.5 and 2.5, the mean being 1.3.

HO_x in the Upper Troposphere

Figure 1 shows a comparison between observations and diel steady state model calculations of the OH and HO₂ mixing ratios in the upper troposphere (8-12.5 km). OH and HO₂ were detected by laser induced fluorescence with a 50% uncertainty [Brune *et al.*, this issue]. OH was measured between April 20 and May 15, 1996. Simultaneous HO₂ observations became available starting May 2. The steady state model generally underestimates the observed HO₂ and OH. The level of agreement varies on a flight to flight basis: the mean ratio of observed-to-modeled HO₂ ranged between 0.85 and 3.6. For OH this mean ratio ranged between 0.75 and 2.8. Much better agreement was found for the HO₂/OH ratio, which reflects rapid cycling between OH and HO₂ driven principally by CO and NO. Simulated HO₂/OH ratios were generally within 20-30% of the observations [Brune *et al.*, this issue]. During a few flights, air with a strong stratospheric signature was sampled (O₃ > 300 ppbv). On these occasions, observed and modeled HO_x were within 10-30% of each other.

The primary sources of HO_x in the diel steady state model include the reaction of O(¹D) with water vapor and, in the upper troposphere, acetone photolysis [Singh *et al.*, 1995]. For the conditions of SUCCESS, acetone photolysis becomes an important primary source of HO_x when water vapor falls below 100 ppmv. The average water vapor mixing ratio measured above 10 km during SUCCESS was 60 ppmv. Thus, not including acetone results in even larger underpredictions of the observed HO_x than shown in Figure 1 [Brune *et al.*, this issue]. The uncertainty associated with the acetone concentrations in SUCCESS is buffered by the quadratic loss of HO_x through the reaction OH+HO₂. If the actual acetone concentrations were a factor of two larger than assumed (average of 1100 pptv instead of 550 pptv), the resulting HO_x concentrations would be at most 50% larger than in the calculations presented here. This would still be lower than observed.

Our analysis of the NO_x data in SUCCESS [Jaeglé *et al.*, this issue] shows that convection of boundary layer air frequently supplied fresh NO_x to the upper troposphere, resulting in observed NO_x/NO_y concentrations ratios higher than predicted from chemical steady state. Convection of boundary layer air can also supply elevated levels of peroxides (CH₃OOH and H₂O₂) and carbonyls (CH₂O) to the upper troposphere [Prather and Jacob, 1997]. Our previous analysis of HO_x measurements made during the STRAT campaign over the North Pacific identified convective injection of peroxides as a potential major source of HO_x in the upper troposphere [Jaeglé *et al.*, 1997].

No observations of peroxides or carbonyls were made during SUCCESS. Our model calculations, assuming these species to be in a chemical steady state defined by the primary sources of HO_x from water vapor and acetone, yield mean concentrations of H₂O₂, CH₃OOH and CH₂O at 10-12 km altitude of 135 ± 110 pptv, 40 ± 36 pptv, and 25 ± 8 pptv respectively. These values can be compared to typical boundary layer concentrations over the United States for that time of year of 400-2800 pptv H₂O₂ [Boatman *et al.*, 1989], 400-700 pptv CH₃OOH [Hewitt and Kok, 1991], and the 500-2700 pptv CH₂O [Hastie *et al.*, 1993; Harris *et al.*, 1989]. The boundary layer concentrations are one order of magnitude higher than the steady state model values in the upper troposphere. Convective injection of boundary layer air could thus be expected to provide a major source of peroxides and CH₂O, and consequently of HO_x, in the upper troposphere. Although H₂O₂ is highly water-soluble and would be efficiently scavenged by the precipitation associated with deep convection, CH₃OOH and CH₂O are only sparingly soluble [Berterton, 1992] and would escape scavenging. Using the HO_x yields per molecule calculated by Prather and Jacob [1997], we find that convective injection of CH₂O could be a source of HO_x comparable to CH₃OOH.

The highest levels of OH in the upper troposphere during SUCCESS were measured on the May 8 flight as the DC-8 sampled the anvil of an active convective system over Wisconsin at an altitude of 11 km. Figure 2 shows the observations of OH, HO₂, NO, NO_y, and condensation nuclei (CN) obtained for this flight as the aircraft flew in and around the anvil. Air impacted by convection is evidenced by high levels of CN (> 1000 cm⁻³) on three occasions along the flight track: 12.9-13.05 hours, 13.7-14.1 hours, and 14.3-14.4 hours. Observations of simultaneously enhanced NO show that convection was accompanied by lightning. This is particularly evident for the second event between local times 13.7 and 14.1 hours, as the aircraft was flying above the anvil: the high levels of NO, up to 1.8 ppbv, represented most of NO_y (NO/NO_y = 0.7 mol/mol). CO was only moderately enhanced during this period (120 ppbv compared to a background of 100 ppbv), which indicates that lightning rather than convec-

tively pumped pollution was the source of elevated NO. Note the high NO_y concentrations measured between times 13.05 and 13.2 hours, with relatively low NO. Stratospheric air was sampled on that occasion: high concentrations of O₃, and low concentrations of N₂O and CH₄ were simultaneously observed.

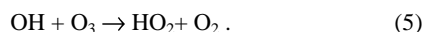
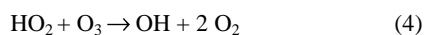
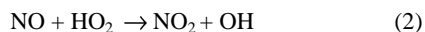
Observed concentrations of OH and HO₂ show considerable variability along the flight track (Figure 2). Part of this variability is due to changes in NO and thus in the HO₂/OH ratio, and part of it can also be due to changes in the UV flux as the aircraft flew in the vicinity of the anvil. Also shown in the figure are the diel steady state model calculations along the flight track. While the model calculations are within 10-40% of the observations between times 13.0 and 13.7 hours, above the anvil (13.7-14.1 hours) they underestimate OH by a factor of 2 and HO₂ by a factor of 4. Adding 500-1000 pptv of CH₃OOH+H₂O₂+CH₂O to the model (compared to 20-200 pptv at steady state) can reconcile model and observations. As noted earlier, observations in the boundary layer show 1300-6200 pptv of CH₃OOH+H₂O₂+CH₂O. Thus in order to account for the observed HO_x levels, less than a 20% fraction of these peroxides needs to have been transported to the upper troposphere through the convective event. We conclude that the frequent convective injection of peroxides and formaldehyde is a tenable explanation to account for the high levels of HO_x observed on May 8 and on other flights in SUCCESS.

Ozone Production

The net ozone production in the upper troposphere is given to a close approximation by (e.g. *Davis et al.*, 1996):

$$P(\text{O}_3) - L(\text{O}_3) = k_2 [\text{NO}][\text{HO}_2] - (k_3 [\text{O}({}^1\text{D})][\text{H}_2\text{O}] + k_4 [\text{HO}_2][\text{O}_3] + k_5 [\text{OH}][\text{O}_3]) \quad (1)$$

where k_2 , k_3 , k_4 , and k_5 are the rate constants for the reactions



The source of ozone from reactions of peroxy radicals (RO₂) with NO is neglected in equation (1) because it makes only a small contribution to ozone production in the upper troposphere [*Davis et al.*, 1996]. When we compare the results from equation (1) to the more complete ozone production rates calculated in our 0-D model, we find that agreement is better than 20%. In the upper troposphere, the ozone loss from reactions (3)-(5) is generally less than 20% of the ozone production from reaction (2).

From equation (1) we calculate the instantaneous net ozone production along the SUCCESS flight tracks solely on the basis of the observed NO, HO₂, OH, O₃ and H₂O concentrations; we then scale these instantaneous rates to 24-hour average values by using the relationship between instantaneous and 24-hour average rates as calculated from the 0-D model. The resulting ozone production rates are shown in Figure 3 (red circles) as a function of the local NO_x concentrations (measured NO plus model-calculated NO₂). Observations made in fresh aircraft exhaust plumes (CO₂ > 368 ppmv and NO > 300 pptv) and in the stratosphere (N₂O < 310 ppbv and O₃ > 100 ppbv) were excluded from this figure. Ozone production rates calculated from the 0-D diel steady state model (blue pluses) are shown for comparison. The dashed line in Figure 3 (case 1) shows the calculated dependence of the net ozone production on NO_x for a set of steady state cal-

culations where all model input variables were specified from average conditions observed in SUCCESS at 11 km ($O_3 = 65$ ppbv; $H_2O = 60$ ppmv; $CO = 120$ ppbv; $CH_4 = 1750$ ppbv; temperature = 217 K). The mean acetone concentration used was 510 pptv. For comparison, we also show the net ozone production for calculations without the source of HO_x from acetone (dotted line in Figure 3, case 0).

As we saw in the previous section the 0-D model generally underestimates the HO_x observations possibly because of a missing source from convective injection of peroxides and CH_2O . The solid line in Figure 3 (case 2) shows model results for the previously described average conditions but with added convective sources of 1×10^4 molecules $cm^{-3}s^{-1}$ H_2O_2 , 4×10^4 molecules $cm^{-3}s^{-1}$ CH_3OOH , and 4×10^4 molecules $cm^{-3}s^{-1}$ CH_2O . These sources result in 2000-500 pptv of H_2O_2 , 1000-150 pptv of CH_3OOH , and 90-120 pptv of CH_2O , depending on the levels of NO_x . These concentrations are higher than their steady state predicted values (H_2O_2 : 210-10 pptv; CH_3OOH : 130-10 pptv, and CH_2O : 10-35 pptv).

Ozone production increases with increasing NO_x (NO_x -limited regime) up to a maximum NO_x value beyond which it decreases (NO_x -saturated regime). Whether ozone production is NO_x -limited or NO_x -saturated depends on the HO_x loss pathways. For high NO_x values, loss of HO_x mainly occurs through the formation of HNO_3 and HNO_4 followed by their reaction with OH. For lower NO_x values, loss of HO_x is dominated by the reaction of OH with HO_2 .

Figure 3 shows that the high levels of observed HO_x , as compared to a standard photochemical model, result in more active ozone production and a steeper increase in ozone production for a given increase in NO_x . This dependence can be reproduced in our box model calculation for average SUCCESS conditions at 11 km by assuming a convective source of peroxides and CH_2O (case 2). As a result of the elevated levels of HO_x , the NO_x -limited regime is extended from 490 pptv (case 1) to 700 pptv of NO_x (case 2). In the study by *Brasseur et al.* [1996], the turnover point for NO_x in the upper troposphere was found to be at a lower value of 280 pptv. Neither acetone nor convective injection of peroxides and carbonyls were included in that study.

The mean NO_x mixing ratio observed in the upper troposphere during SUCCESS was 70 pptv, corresponding to an average net ozone production rate of 2 ppbv/day which is twice the rate calculated with the steady state model. Ozone production was NO_x -limited under all essentially all conditions encountered in SUCCESS. When the DC-8 sampled lightning affected air on May 8, we calculate very elevated ozone production rates (>8 ppbv day^{-1} , shown by arrows in Figure 3) based on the observed HO_x and NO. For this time interval, the steady state model predicts low ozone production because of NO_x -saturated conditions. It appears that the enhanced supply HO_x from convection increases the effectiveness of lightning NO_x as a source of ozone.

A more general picture of the dependence of ozone production on NO_x and HO_x production is shown in Figure 4. This figure was constructed by varying both the NO_x concentrations and the HO_x primary sources in the steady state model applied to the average SUCCESS conditions at 11 km altitude. The primary sources of HO_x include the $O(^1D)+H_2O$ reaction and the photolysis of acetone. In addition, we have added a varying source from convective injection of peroxides and formaldehyde. All these sources have been weighted by their yield in HO_x molecules. The three curves shown in Figure 3 (cases 0, 1, and 2) are reproduced in Figure 4. The HO_x yield from acetone is a strong function of NO, while the yields from $O(^1D)+H_2O$, H_2O_2 , CH_3OOH , and CH_2O are relatively independent of NO. As a result, the

HO_x source in case 1, which is dominated by acetone, varies with NO_x even though the acetone mixing ratio remains constant.

The dashed-dotted line in the Figure separates the NO_x-limited and NO_x-saturated regimes. Over the range of HO_x source rates expected in the upper troposphere (10^3 - 5×10^5 molecules cm⁻³s⁻¹), the turnover point between the two regimes varies between 350 and 1200 pptv of NO_x. Aircraft observations of NO_x in the upper troposphere worldwide [Bradshaw *et al.*, 1997] are consistently lower than these turnover points, indicating that ozone production is NO_x-limited. We also see from Figure 4 that ozone production in the upper troposphere is insensitive to the supply of HO_x when NO_x is below 30 pptv. Such low values are rarely observed in the upper troposphere except in the outflow of deep marine convection in the tropics where lightning generally does not take place [Bradshaw *et al.*, 1997]. Enhancement of peroxides in the outflow of deep marine convection thus leads to little increase of ozone production [Folkins *et al.*, manuscript in preparation, 1997]. Considerable increase of ozone production may however be expected from enhanced peroxides and CH₂O in continental convection associated with lightning. Figure 4 illustrates how our ability to model the extent of human influence on ozone in the upper troposphere relies on how well we simulate the levels of both NO_x and HO_x.

Acknowledgments. The authors would like to thank A. J. Miller and C. Long for making available the ozone SBUV/2 data; B. Anderson for providing the Eppley radiometer data; D. Hagen for the CN observations; and two anonymous reviewers for their helpful comments. This work was supported by the National Aeronautics and Space Administration (NASA-NAG5-2688).

References

- Betterton, E.A., Henry's law constants of soluble and moderately soluble organic gases: Effects on aqueous phase chemistry, *Adv. Environ. Sci. Technol.*, 24, 1-50, 1992.
- Boatman, J.F., *et al.*, Airborne sampling of selected trace chemicals above the central United States, *J. Geophys. Res.*, 94, 5081-5093, 1989.
- Bradshaw, J.D., *et al.*, On the observed distributions of nitrogen oxides in the remote free troposphere, *Rev. Geophys.*, *in press*, 1997.
- Brasseur, G.P., *et al.*, Atmospheric impact of NO_x emissions by subsonic aircraft: a three-dimensional model study, *J. Geophys. Res.*, 101, 1423-1428, 1996.
- Brune, W.H., *et al.*, Airborne in situ OH and HO₂ observations in the cloud-free troposphere and lower stratosphere during SUCCESS, *Geophys. Res. Lett.*, this issue.
- Campos, T.L., *et al.*, Measurements of NO and NO_y emission indices during SUCCESS, *Geophys. Res. Lett.*, this issue.
- Davis, D.D., *et al.*, Assessment of ozone photochemistry in the western North Pacific as inferred from PEM-West A observations during the fall 1991, *J. Geophys. Res.*, 101, 2111-2134, 1996.
- DeMore, W.B., *et al.*, Chemical kinetics and photochemical data for use in stratospheric modeling, *Jet Propul. Lab. Publ.* 97-4, 1997.
- Harris, G.W., *et al.*, Measurements of formaldehyde in the troposphere by tunable diode laser absorption spectroscopy, *J. Atmos. Chem.*, 8, 119-137, 1989.
- Hastie, D.R., *et al.*, The influence of the nocturnal boundary layer on secondary trace species in the atmosphere at Dorset, Ontario, *Atmos. Environ.*, 27, 533-541, 1993.
- Hewitt, C.N., and G.L. Kok, Formation and occurrence of organic hydroperoxides in the troposphere laboratory and field observations, *J. Atmos. Chem.*, 12, 181-194, 1991.
- Jacob, D.J., *et al.*, The origin of ozone and NO_x in the tropical troposphere: a photochemical analysis of aircraft observations over the South Atlantic Basin, *J. Geophys. Res.*, 101, 24,235-34,250, 1996.
- Jaeglé, L., *et al.*, Sources and chemistry of NO_x in the upper troposphere above the United States, *Geophys. Res. Lett.*, this issue.

- Jaeglé, L., *et al.*, Observations of OH and HO₂ in the upper troposphere suggest a strong source from convective injection of peroxides, *Geophys. Res. Lett.*, *in press*, 1997.
- Madronich, S., Intercomparison of NO₂ photodissociation and UV radiometer measurements, *Atmos. Environ.*, *21*, 569-578, 1987.
- McKeen, S.A., *et al.*, The photochemistry of acetone in the upper troposphere: a source of odd-hydrogen radicals, *Geophys. Res. Lett.*, *in press*, 1997.
- National Aeronautics and Space Administration, Atmospheric effects of aviation: Interim assessment report of the advanced subsonic technology program, *Ref. Publ. 1400*, 1997.
- Prather, M.J., and D.J. Jacob, A persistent imbalance in HO_x and NO_x photochemistry of the upper troposphere driven by deep tropical convection, submitted to *Geophys. Res. Lett.*, 1997.
- Schumann, U., Editor, AERONOX - The impact of NO_x emissions from aircraft upon the atmosphere at flight altitude 8-15 km, *Report EUR 16209 EN, European Commission DG XXII and DLR Cologne*, 1995.
- Singh, H.B., *et al.*, High concentrations and photochemical fate of oxygenated hydrocarbons in the global troposphere, *Nature*, *378*, 50-54, 1995.
- Toon, O.B., *et al.*, Overview of SUCCESS, *Geophys. Res. Lett.*, this issue.

W.B. Brune, I. Faloon, D. Tan, Pennsylvania State University, Department of Meteorology, University Park, PA 16802.

T.L. Campos, B.A. Ridley, A.J. Weinheimer, Atmospheric Chemistry Division, NCAR, Boulder, CO 80307.

D.J. Jacob, L. Jaeglé (corresponding author), Department of Earth and Planetary Sciences, Harvard University, 29 Oxford Street, Pierce Hall, Cambridge, MA 02138. (e-mail: lj@io.harvard.edu)

G.W. Sachse, NASA Langley Research Center, Hampton, VA 23681.

(Received _____; revised _____;
accepted: _____)

¹Harvard University, Cambridge, Massachusetts.

²Pennsylvania State University, University Park.

³NCAR, Boulder, Colorado.

⁴NASA Langley Research Center, Hampton, Virginia.

JAEGLÉ ET AL.: HO_x SOURCES AND O₃ PRODUCTION

JAEGLÉ ET AL.: HO_x SOURCES AND O₃ PRODUCTION

JAEGLÉ ET AL.: HO_x SOURCES AND O₃ PRODUCTION

Figure 1. Comparison between observations and steady state model calculations of HO₂ and OH mixing ratios for the SUCCESS flights between April 20 and May 15, 1996 in the upper troposphere (8-12.5 km altitude). The model was sampled at the time of day of the observations. HO₂ data was only available for the May flights. Also shown are the 1:1 lines. Observations in aircraft exhaust plumes have been excluded from this figure.

Figure 2. Data from a SUCCESS flight in and around a meso-scale convective system over Wisconsin on May 8, 1996. The altitude varied between 11 and 12 km. Observations of (a) condensation nuclei, (b) NO (solid circles) and NO_y (pluses), (c) OH and (d) HO₂, are shown along the flight track as a function of local time. Steady state model calculations (solid lines) are also shown for OH and HO₂.

Figure 3. Net ozone production (24-hour average) as a function of NO_x above 8 km: comparison between steady state point model calculations (blue pluses) and observations (red solid circles). The observed rates were computed from measured concentrations of HO₂, OH, and NO, and scaled to 24-hour average

values using diel factors from the photochemical model (see text). Observations made in fresh aircraft exhaust plumes and in the stratosphere are excluded from this figure. The three curves show model calculations for average conditions during SUCCESS at 11 km, assuming different levels of HO_x source. The dashed line (case 1) assumes the peroxides and formaldehyde to be at steady state, while the solid line (case 2) assumes a convective source of peroxides and formaldehyde. The dotted line (case 0) is the same as case 1 but without production of HO_x from acetone photolysis. The NO_x concentration is the sum of observed NO and model-calculated NO₂ (chemical steady state).

Figure 4. Contour plot of 24-hour average ozone production (in ppbv day⁻¹) in the upper troposphere as a function of the NO_x concentrations and the primary HO_x production rate. Primary HO_x production includes the sources from O(¹D)+H₂O, acetone photolysis, and deep convective injection of peroxides and carbonyls. These sources have been weighted by their yields in HO_x molecules. The O₃ production rates were calculated from equation (1) with a 0-D model for average conditions during SUCCESS at 11 km altitude. The three model cases shown in Figure 3 are reproduced here as dotted (case 0), solid (case 1), and dashed lines (case 2). The transition between the NO_x-limited and NO_x-saturated regimes is shown by the dashed-dotted line.

Figure 1. Comparison between observations and steady state model calculations of HO₂ and OH mixing ratios for the SUCCESS flights between April 20 and May 15, 1996 in the upper troposphere (8-12.5 km altitude). The model was sampled at the time of day of the observations. HO₂ data was only available for the May flights. Also shown are the 1:1 lines. Observations in aircraft exhaust plumes have been excluded from this figure.

Figure 2. Data from a SUCCESS flight in and around a mesoscale convective system over Wisconsin on May 8, 1996. The altitude varied between 11 and 12 km. Observations of (a) condensation nuclei, (b) NO (solid circles) and NO_y (pluses), (c) OH and (d) HO₂, are shown along the flight track as a function of local time. Steady state model calculations (solid lines) are also shown for OH and HO₂.

Figure 3. Net ozone production (24-hour average) as a function of NO_x above 8 km: comparison between steady state point model calculations (blue pluses) and observations (red solid circles). The observed rates were computed from measured concentrations of HO₂, OH, and NO, and scaled to 24-hour average values using diel factors from the photochemical model (see text). Observations made in fresh aircraft exhaust plumes and in the stratosphere are excluded from this figure. The three curves show model calculations for average conditions during SUCCESS at 11 km, assuming different levels of HO_x source. The dashed line (case 1) assumes the peroxides and formaldehyde to be at steady state, while the solid line (case 2) assumes a convective source of peroxides and formaldehyde. The dotted line (case 0) is the same as case 1 but without production of HO_x from acetone photolysis. The NO_x concentration is the sum of observed NO and model-calculated NO₂ (chemical steady state).

Figure 4. Contour plot of 24-hour average ozone production (in ppbv day⁻¹) in the upper troposphere as a function of the NO_x concentrations and the primary HO_x production rate. Primary HO_x production includes the sources from O(¹D)+H₂O, acetone photolysis, and deep convective injection of peroxides and carbonyls. These sources have been weighted by their yields in HO_x molecules. The O₃ production rates were calculated from equation (1) with a 0-D model for average conditions during SUCCESS at 11 km altitude. The three model cases shown in Figure 3 are reproduced here as dotted (case 0), solid (case 1), and dashed lines (case 2). The transition between the NO_x-limited and NO_x-saturated regimes is shown by the dashed-dotted line.